

# Characteristics of Corn Grains Pyrolysis in a Fixed Bed Reactor

OANA CRISTINA PARVULESCU<sup>1\*</sup> TANASE DOBRE, LAURENȚIU CEATRA, GUSTAV IAVORSHI, RADU MIREA

University „Politehnica” of Bucharest, Chemical Engineering Department, 1-3 Polizu, 011061, Bucharest, Romania

*Corn grains pyrolysis was performed in a fixed bed reactor under carbon dioxide atmosphere, producing a char, pyrolytic oil and incondensable gases. The distribution of these fractions was dependent on variations in heat flux, carbon dioxide superficial velocity and grain size. A 2<sup>3</sup> factorial experiment was employed in order to establish correlations between these factors and process dependent variables, namely char mass, oil mass, operation time, material bed centre temperature, reactor wall temperature and volatiles temperature. A one-stage global reaction kinetic model was selected to describe the process dynamics and its parameters were estimated based on experimental data. The research results may provide useful data to design, scale-up and operate the fixed bed pyrolysis reactors.*

*Keywords: pyrolysis, corn, biomass, factorial experiment, kinetic model*

Vegetal materials are abundant, clean and cheap sources of renewable energy with a great potential to replace conventional fossil fuels. They can be converted into convenient solid, liquid and gaseous fuels by thermo-chemical and biological conversion technologies. The thermo-chemical processes, such as pyrolysis, gasification and combustion, lead to lower emissions of SO<sub>2</sub>, NO<sub>x</sub> and soot, due to negligible content of sulphur, nitrogen and ash of vegetal materials. Reduced amounts of CO<sub>2</sub> are achieved because a part of CO<sub>2</sub> released by conversion will be recycled into the plants by photosynthesis. Vegetal materials resources include wood and wood wastes, agricultural crops and their waste by-products, wastes from food processing, aquatic plants, algae etc. They contain cellulose, hemicellulose, lignin, starch, lipids, proteins, simple sugars, water, ash and other compounds.

Vegetal materials pyrolysis, consisting of solid thermal degradation without oxygen, is usually performed in presence of a carrier gas which can be inert (nitrogen, argon) or oxidant (carbon dioxide, steam). The pyrolysis products are lumped into three groups: permanent gases, a pyrolytic liquid (bio-oil/tar) and a solid residue (char), or simply into volatiles and char. Their distribution and composition depend on raw material properties (chemical composition, size, shape, density), nature and flow rate of carrier gas, heating rate, process temperature, operation time, reactor type etc [1-16]. These products result from both primary decomposition reactions of the solid material and secondary degradation reactions of the condensable volatile organic compounds into char and low molecular weight gases, as they are transported through the reaction environment [3,4,11]. The pyrolytic gas and bio-oil can be employed as combustibles or raw materials sources, whereas the char is useful as a renewable fuel, active carbon or catalyst support.

This paper focuses on the qualitative and quantitative characterization of fixed bed pyrolysis of corn grains, in the presence of a carbon dioxide stream.

## Experimental part

### Materials

Crushed corn grains were employed as a vegetal material. Two fractions of grain size, with a mean volume equivalent diameter of 0.2 cm and 0.4 cm, were selected for subsequent studies. The mean percentage composition of a corn grain is listed in table 1.

The cross section of a corn grain shown in figure 1 reveals its main parts, i.e. hull, tip cap, germ and endosperm. The hull and tip cap, accounting for about 6-8% of the grain weight, have a high content of fibers ( $\approx$  90 %). The germ (embryo), in which most of the fats resides, is about 10-12%. The remainder of the grain is endosperm which consists of 85-90% starch, 8-10% proteins (gluten) and a small amount of fats and other compounds [18]. In endosperm the starch granules are encased in a continuous proteins matrix. Characteristic gluten matrix of horny endosperm is very dense and the starch particles are held more firmly, whereas in floury endosperm the matrix is less dense and starch granules are dispersed loosely. Accordingly, the starch granules in floury endosperm can be degraded easier than in horny endosperm.

### Equipment and procedure

The laboratory set-up (fig. 2) used for experimental investigation of corn grains pyrolysis is the same employed in our previous studies [19-22]. The vegetal material is introduced in a pyrolysis oven (PO), whose main part is a column (1), which is made from quartz, 50 mm diameter and 500 mm height, set into a fixed support (5) and equipped with a cup (6) and a gasket (7). The column wall, thermally isolated by glass fibre isolation (2) and glass cylinder with reflectorized internal surface (3), is heated by an electric resistance (4), which is fed by an autotransformer (17); accordingly, the vegetal material bed (13) is heated and thermally decomposed.

The carbon dioxide from cylinder (20), whose flow is measured by a flow-meter (18) and regulated by a pressure

**Table 1**  
COMPOSITION OF A CORN GRAIN [17]

Compound	Starch	Proteins	Fibers	Fats	Sugars	Ash	Water
% wt.	62.7	8.2	8.2	3.7	2.2	1.2	13.8

\* email: oana.parvulescu@yahoo.com; Tel.: (+40) 021 402 38 10

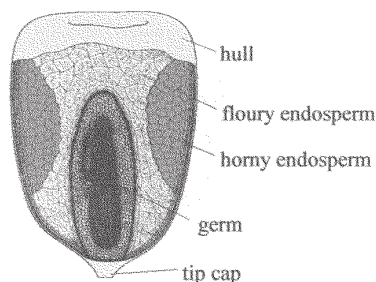


Fig. 1. Structure of a corn grain [18]

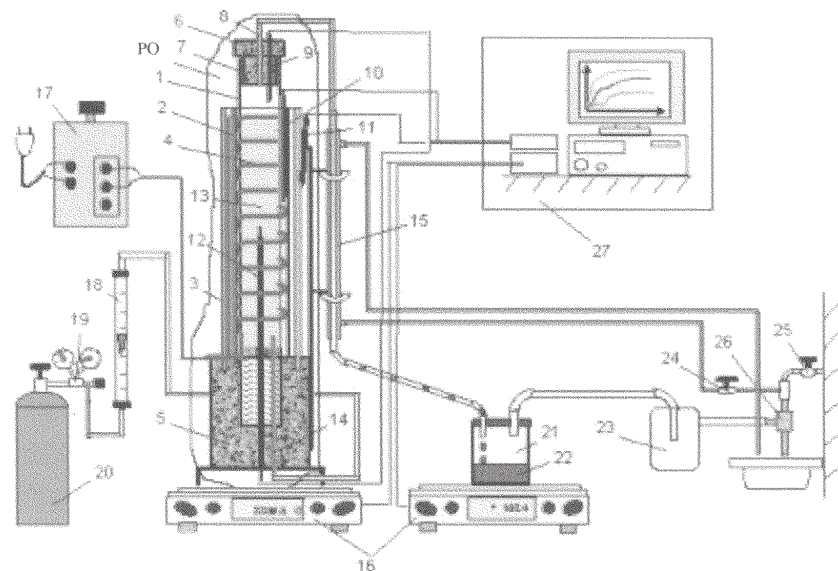


Fig. 2. Experimental set-up:

(PO) pyrolysis oven; (1) quartz column; (2) glass fibre isolation; (3) glass cylinder with reflectorized internal surface; (4) electric resistance; (5) ceramic support; (6) ceramic cap; (7) asbestos gasket; (8) volatiles collector; (9)-(12) thermocouples; (13) vegetal material bed; (14) carbon dioxide feed pipe; (15) condenser; (16) electronic balances; (17) autotransformer; (18) flow-meter; (19) pressure reducer; (20) carbon dioxide cylinder; (21) oil collector; (22) oil; (23) drops separator; (24), (25) valves; (26) suction pump; (27) data acquisition system

reducer (19), is introduced into the oven by a pipe (14), up-flows through the material fixed bed and is evacuated by a collector (8) with the volatiles obtained during the pyrolysis. The mixture of gases and vapours is cooled in a condenser (15), producing pyrolytic oil (22) and incondensable gases. The oil is collected in a vessel (21) and the incondensable gases are removed through the upper part of vessel (21), passed to a drops separator (23) and then evacuated by a suction pump (26).

The temperatures in certain zones are measured by the thermocouples (9)-(12). Vegetal material and oil masses are recorded on-line by the electronic balances (16). All the data are collected by an acquisition system (27).

### Experimental variables

Experimental investigation was conducted at two values (levels) of heat flux,  $q$ , carbon dioxide superficial velocity,  $w$ , and mean volume equivalent diameter of corn grain,  $d$ . A set of 8 experiences were carried out according to a  $2^3$  factorial plan. Vegetal material mass,  $m$ , oil mass,  $m_{oil}$ , bed centre temperature,  $t_c$ , column wall temperature,  $t_w$ , and volatiles temperature,  $t_v$ , were continuously recorded as a function of heating time,  $\tau$ . Each experience was replicated three times to determine its reproducibility, which was found to be good.

## Results and discussion

### Pyrolysis experimental curves

Process independent variables (factors) levels for the experiences performed are summarized in table 2.

Experimental results concerning the pyrolysis dynamics are given in figures 3 and 4. Time variation curves of vegetal material bed mass,  $m/m_0$ , and oil mass,  $m_{oil}/m_0$ , illustrated in figure 3, have the same shape of bent step. They are correlated by cause-effect type relationship, the oil mass increase in figure 3b being an effect of the material mass decrease in figure a. As expected, a decrease in char yield and an enlargement of oil production occur at high value of heat flux.

Table 2

PROCESS FACTORS LEVELS

Exp.	$q$ (W/m <sup>2</sup> )	$w$ (m/h)	$d$ (cm)
1	2600	1	0.2
2	2600	2	0.2
3	3470	1	0.2
4	3470	2	0.2
5	2600	1	0.4
6	2600	2	0.4
7	3470	1	0.4
8	3470	2	0.4

A decrease in oil mass with carbon dioxide velocity increasing is emphasized in figure 3b. This is probably due to a shorter residence time of the volatiles in the condenser, producing the condensation of a smaller vapour amount. Grain size can be an important variable that affects the process. Accordingly, an increase in grain size may determine temperature gradients in the particle, so the temperature at the centre can be lower than that at the surface, resulting an increase in solid amount and a decrease in oil production [11,15,22]. The mass curves presented in figure 3 reveal a slight influence of grain size on the pyrolysis products yield. Consequently, it can be assumed that with grains less than 0.4 cm there was no temperature gradient, which could lead to heat transfer problems.

Figure 4, which shows temperature dynamics of bed centre,  $t_c$ , column wall,  $t_w$ , and volatiles,  $t_v$ , indicates that temperatures increase with heat flux increasing and are almost invariant with gas velocity and grain size. Wall temperature dynamics (fig. 4b) reveal an unsteady state heating accompanied by endothermic decomposition reactions of the volatile compounds. Each volatiles temperature curve (fig. 4c) presents a maximum temperature value and these maximum values appear earlier at high value of heat flux.

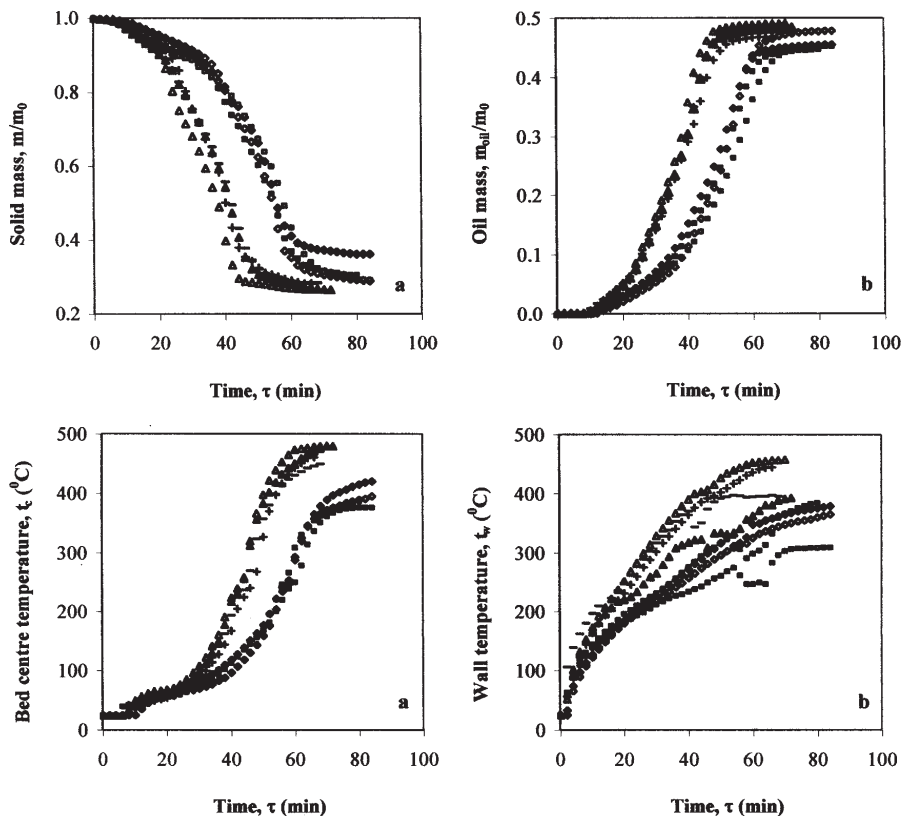


Fig. 3. Time variation of mass of: a) vegetative material; b) pyrolytic oil ( $\blacklozenge$  exp 1,  $\blacksquare$  exp 2,  $\blacktriangle$  exp 3,  $-$  exp 4,  $\diamond$  exp 5,  $\square$  exp 6,  $\Delta$  exp 7,  $+$  exp 8)

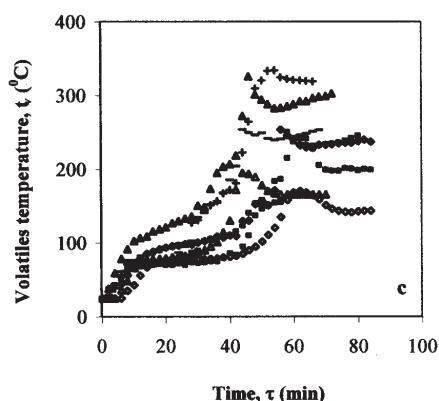


Fig. 4. Time variation of temperature of: a) material bed centre; b) column wall; c) volatiles ( $\blacklozenge$  exp 1,  $\blacksquare$  exp 2,  $\blacktriangle$  exp 3,  $-$  exp 4,  $\diamond$  exp 5,  $\square$  exp 6,  $\Delta$  exp 7,  $+$  exp 8)

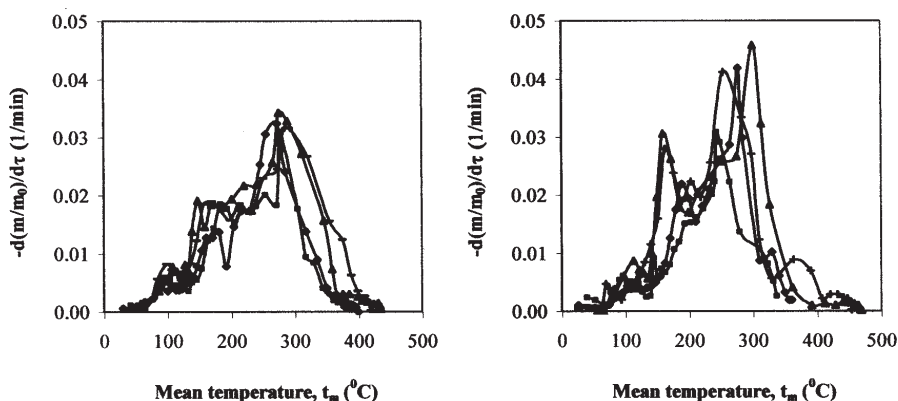


Fig. 5. Mass loss rate versus logarithmic mean temperature ( $\blacklozenge$  exp 1,  $\blacksquare$  exp 2,  $\blacktriangle$  exp 3,  $-$  exp 4,  $\diamond$  exp 5,  $\square$  exp 6,  $\Delta$  exp 7,  $+$  exp 8)

Figure 5 illustrates material mass loss rate,  $\frac{d(m/m_0)}{d\tau}$  depending on logarithmic mean temperature between bed centre and column wall,  $t_m$ . Each differential curve in figure 5 has two relevant peaks, emphasizing that the pyrolysis develops intensely in two main stages. The first stage, characterized by smaller peak amplitudes and temperatures range between 144 and 188°C, can be attributed to the starch degradation in floury endosperm,

whereas the second stage, with higher peaks amplitude and temperatures between 243 and 299°C, can be an effect of the starch degradation in horny endosperm.

The values of maximum material loss rate,  $\left[ \frac{d(m/m_0)}{d\tau} \right]_{peak}$ , and of corresponding logarithmic mean temperature,  $(t_{m,peak})$ , for the both degradation stages under various operation conditions, are summarized in table 3.

Exp.	$\left[ \frac{d(m/m_0)}{d\tau} \right]_{peak}$ (1/min)		$(t_m)_{peak}$ (°C)	
	1 <sup>st</sup> stage	2 <sup>nd</sup> stage	1 <sup>st</sup> stage	2 <sup>nd</sup> stage
1	0.014	0.032	180	272
2	0.019	0.031	182	278
3	0.019	0.034	146	274
4	0.019	0.032	169	290
5	0.022	0.042	188	277
6	0.009	0.031	144	243
7	0.031	0.046	159	299
8	0.028	0.041	162	253

**Table 3**  
MAXIMUM MATERIAL LOSS RATE AND  
CORRESPONDING  
PEAK TEMPERATURE

Exp.	$x_1$	$x_2$	$x_3$	$y_1$	$y_2$	$y_3$ (min/g)	$y_4$ (°C/g)	$y_5$ (°C/g)	$y_6$ (°C/g)
1	-1	-1	-1	0.362	0.455	0.266	1.327	1.200	0.750
2	-1	1	-1	0.305	0.447	0.253	1.224	1.215	0.775
3	1	-1	-1	0.266	0.483	0.235	1.516	1.242	0.958
4	1	1	-1	0.285	0.478	0.215	1.420	1.251	0.800
5	-1	-1	1	0.285	0.480	0.265	1.185	1.091	0.428
6	-1	1	1	0.293	0.453	0.253	1.106	0.911	0.587
7	1	-1	1	0.267	0.491	0.206	1.412	1.345	0.489
8	1	1	1	0.283	0.469	0.194	1.353	1.307	0.938

**Table 4**  
EXPERIMENTAL MATRIX

Characteristic data of the second peak listed in table 3 show that the peak height and the corresponding temperature are greater at high value of heat flux, in compliance with the data reported in the related literature [1,6,7,9,10,15].

#### Factorial experiment

Vegetal material mass,  $m$ , oil mass,  $m_{oil}$ , operation time,  $\tau$ , material bed centre temperature,  $t_c$ , column wall temperature,  $t_w$ , and volatiles temperature,  $t_v$ , were selected as process dependent variables (responses). These variables can be linked to the process factors by adequate equations. Factors dimensionless values were calculated depending on natural values with the following correlations:

$$x_1 = \frac{q - 3035}{435} \quad (1)$$

$$x_2 = \frac{w - 1.5}{0.5} \quad (2)$$

$$x_3 = \frac{d - 0.3}{0.1} \quad (3)$$

Factors dimensionless values as well as responses final values divided by the initial material mass, namely  $y_1 = \frac{m_f}{m_0}$ ,  $y_2 = \frac{m_{oilf}}{m_0}$ ,  $y_3 = \frac{\tau_f}{m_0}$ ,  $y_4 = \frac{t_{cf}}{m_0}$ ,  $y_5 = \frac{t_{wf}}{m_0}$  and  $y_6 = \frac{t_{vf}}{m_0}$  are given in table 4. Processing the data listed in table 4 based on the procedure recommended for a factorial experiment with 2 levels [23], the following correlations were obtained:

$$y_1 = 0.293 - 0.018x_1 - 0.002x_2 - 0.011x_3 + 0.010x_1x_2 + 0.011x_1x_3 + 0.008x_2x_3 - 0.009x_1x_2x_3 \quad (4)$$

$$y_2 = 0.469 + 0.011x_1 - 0.008x_2 + 0.004x_3 + 0.001x_1x_2 - 0.004x_1x_3 - 0.005x_2x_3 \quad (5)$$

$$y_3 = 0.236 - 0.023x_1 - 0.007x_2 - 0.006x_3 - 0.001x_1x_2 - 0.006x_1x_3 + 0.001x_2x_3 + 0.001x_1x_2x_3 \quad (6)$$

$$y_4 = 1.318 + 0.107x_1 - 0.042x_2 - 0.054x_3 + 0.003x_1x_2 + 0.011x_1x_3 + 0.008x_2x_3 + 0.002x_1x_2x_3 \quad (7)$$

$$y_5 = 1.195 + 0.091x_1 - 0.024x_2 - 0.032x_3 + 0.017x_1x_2 + 0.071x_1x_3 - 0.030x_2x_3 + 0.019x_1x_2x_3 \quad (8)$$

$$y_6 = 0.716 + 0.081x_1 + 0.059x_2 - 0.105x_3 + 0.013x_1x_2 + 0.022x_1x_3 - 0.093x_2x_3 + 0.059x_1x_2x_3 \quad (9)$$

According to figures 3 and 4, eqs. (4)-(9) emphasize that:  
 -final values of solid mass,  $y_1$ , are minimum and of oil mass,  $y_2$ , are maximum for superior level of heat flux,  $x_1$ ;  
 -minimum final values of operation time,  $y_3$ , are achieved for superior level of all factors;  
 -final values of bed centre temperature,  $y_4$ , are maximum for superior level of heat flux,  $x_1$ , as well as for inferior level of carbon dioxide superficial velocity,  $x_2$ , and grain size,  $x_3$ ;  
 -final values of column wall temperature,  $y_5$ , and volatiles temperature,  $y_6$ , are maximum for superior level of  $x_1$ .

**Table 5**  
KINETIC PARAMETERS FOR THE FIRST DECOMPOSITION STAGE

Exp.	$\beta = dT_m/dt$ (K/min)	$t_m$ (°C)	$\alpha$	$A/\beta$ (1/min)	$E$ (kJ/mol)
1	3.09	117-180	0.09-0.35	2318	41.49
2	3.92	120-193	0.12-0.37	6496	45.98
3	3.19	114-168	0.07-0.33	2491	40.34
4	4.84	114-183	0.10-0.34	2122	40.44
5	4.28	146-199	0.13-0.37	201390	69.29
6	3.25	132-184	0.15-0.32	10164	48.81
7	4.55	141-171	0.13-0.34	1414095	62.18
8	4.58	102-175	0.05-0.34	11049	45.33

**Table 6**  
KINETIC PARAMETERS FOR THE SECOND DECOMPOSITION STAGE

Exp.	$\beta = dT_m/dt$ (K/min)	$t_m$ (°C)	$\alpha$	$A/\beta$ (1/min)	$E$ (kJ/mol)
1	6.54	192-285	0.37-0.88	225483	62.39
2	6.43	239-304	0.57-0.91	283226	65.60
3	8.64	219-288	0.49-0.81	5216	47.43
4	8.85	231-319	0.49-0.87	18659	54.26
5	6.48	246-283	0.60-0.88	94112365	90.03
6	4.78	202-279	0.41-0.89	823238	67.66
7	9.37	250-326	0.62-0.96	1111254	71.55
8	9.54	218-298	0.51-0.86	5025	46.02

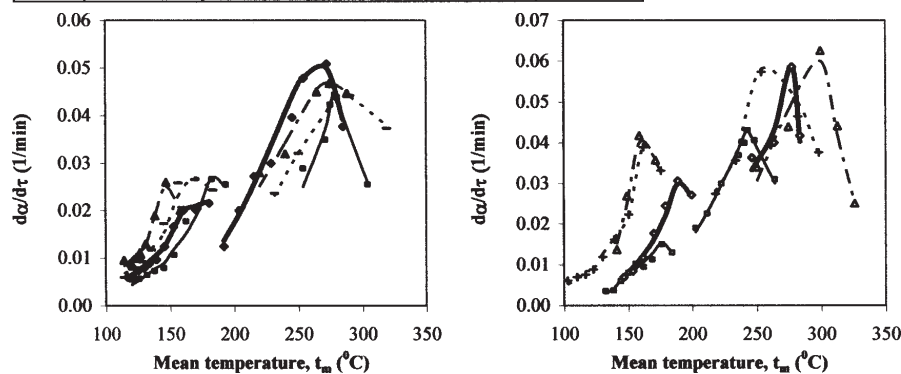


Fig. 6. Comparison between experimental (symbols) and simulated (lines) differential conversion curves  
 (♦ exp 1, ■ exp 2, ▲ exp 3, - exp 4, ◇ exp 5, □ exp 6, Δ exp 7, + exp 8)

### Kinetic model

A one-stage global reaction model was adopted to describe the conversion process from raw material to char and volatiles [1,3,4,6-8,14,15]. For dynamic data obtained at a constant heating rate,  $\beta = \frac{dT_m}{d\tau}$ , the decomposition rate can be described by equation [8]:

$$\frac{d\alpha}{d\tau} = (1-\alpha) \frac{A}{\beta} \exp\left(-\frac{E}{RT_m}\right) \quad (10)$$

where volatiles conversion is expressed as:

$$\alpha = \frac{m_0 - m}{m_0 - m_f} \quad (11)$$

Taking natural logarithms on both sides of Eq. (10) yields:

$$\ln\left[\frac{1}{1-\alpha} \frac{d\alpha}{d\tau}\right] = \ln \frac{A}{\beta} - \frac{E}{RT_m} \quad (12)$$

The values of pre-exponential factor,  $A/\beta$ , and activation energy,  $E$ , for the both decomposition stages, which are summarized in Tables 5 and 6, were obtained from the intercept and the slope of the straight line given by a plot of

$\ln\left[\frac{1}{1-\alpha} \frac{d\alpha}{d\tau}\right]$  versus  $1/T_m$ . Tables 5 and 6 contain also the values of the mean heating rate,  $\beta$ , as well as the ranges of temperature,  $t_m$ , and conversion,  $\alpha$ , wherein these mean values were estimated. As can be seen, the activation energy decreases with heat flux increasing, according to other researches [9,21,22]. Data listed in table 5 show that the pre-exponential factor for the second degradation stage decreases strongly with heat flux increasing.

Figure 6 compares the differential conversion curves predicted by estimated kinetic parameters with the experimental results. A good agreement between experimental and simulated data is proved (errors less than 12 %).

### Conclusions

An experimental set-up was designed and scaled-up in order to study the fixed bed pyrolysis of corn grains. Carbon dioxide was employed as a carrier agent and a reactant in the pyrolysis process. A char, a pyrolytic oil and a gaseous fraction were produced.

A process analysis by  $2^n$  factorial programming was performed, with the factors being heat flux ( $n=1$ ), carbon dioxide superficial velocity ( $n=2$ ) and grain size ( $n=3$ ). Correlations between these factors and process dependent variables, namely char mass, oil mass, operation time, char bed temperature, column wall temperature and volatiles temperature were established.

Under conditions studied, only the heat flux had a significant effect on the process performances. It was found that the pyrolysis develops intensely in two main stages, attributed to the starch decomposition in floury and horny endosperm, respectively. A one-stage global reaction kinetic model, whose parameters were estimated based on experimental data, was selected to simulate the process dynamics. The model predicted well the real conditions and it could facilitate the design, scaling-up and operation of fixed bed pyrolysis reactors.

*Acknowledgements:* This work was supported by CNCISIS-UEFISCU project nr. PN II-IDEI code ID\_1031 (CF 177/2007) and POS-DRU ID project nr. 5159/2008.

### Nomenclature

$A/\beta$  - pre-exponential factor, 1/min  
 $d$  - mean volume equivalent diameter of corn grain, cm  
 $E$  - activation energy, kJ/mol  
 $m$  - vegetal material mass, g  
 $m_{oil}$  - pyrolytic oil mass, g  
 $q$  - heat flux, W/m<sup>2</sup>  
 $R$  - gas universal constant,  $R = 8.314$  J/mol K  
 $t$  - temperature, °C  
 $T$  - absolute temperature, K  
 $w$  - carbon dioxide superficial velocity, m/h  
 $x_i$  - process dimensionless factor,  $i=1..3$   
 $y_j$  - process final response,  $j=1..6$

## Greek letters

$\alpha$  - volatiles conversion

$\beta$  - heating rate,  $\beta = dT_m / dt$ , K/min

$\tau$  - time, min

## Subscripts

$c$  - material bed centre

$f$  - final

$m$  - logarithmic mean

$v$  - volatiles

$w$  - column wall

$0$  - initial

## References

1. ABOULKAS, A., EL HARFI, K., EL BOUADILI, A., NADIFIYINE, M., BENCHANAA, M., MOKHLISSE, A., *Fuel Process. Technol.*, **90**, 2009, p. 722
2. BALAT, M., BALAT, M., KIRTAY, E., BALAT, H., *Energ. Convers. Manage.*, **50**, 2009, p. 3147
3. Di BLASI, C., *J. Anal. Appl. Pyrolysis*, **47**, 1998, p. 43
4. Di BLASI, C., *Prog. Energy Combust. Sci.*, **34**, 2008, p. 47
5. FU, P., HU, S., SUN, L., XIANG, J., YANG, T., ZHANG, A., ZHANG, J., *Biores. Technol.*, **100**, 2009, p. 4877
6. GUINESI, L.S., ROZ, A.L., CORRADINI, E., MATTOSO, L.H.C., TEIXEIRA, E.M., CURVELO, A.A.S., *Thermochim. Acta*, **447**, 2006, p. 190
7. HU, S., JESS, A., XU, M., *Fuel*, **86**, 2007, p. 2778
8. IOANNIDOU, O., ZABANIOTOU, A., *Renew. Sustain. Energ. Rev.*, **11**, 2007, p. 1966
9. JEGUIRIM, M., TROUVE, G., *Biores. Technol.*, **100**, 2009, p. 4026
10. LI, Z., ZHAO, W., MENG, B., LIU, C., ZHU, Q., ZHAO, G., *Biores. Technol.*, **99**, 2008, p. 7616
11. PARIHAR, M.F., KAMIL, M., GOYAL, H.B., GUPTA, A.K., BHATNAGAR, A.K., *Process Saf. Environ. Protect.*, **85**, 2007, p. 458
12. RADMANESH, R., COURBARIAUX, Y., CHAOUKI, J., GUY, C., *Fuel*, **85**, 2006, p. 1211
13. SORUM, L., GRONLI, M.G., HUSTAD, J.E., *Fuel*, **80**, 2001, p. 1217
14. XIU, S., LI, Z., LI, B., YI, W., BAI, X., *Fuel*, **85**, 2006, p. 664
15. YU, F., RUAN, R., STEELE, P., *Trans. ASABE*, **51**, 2008, p. 1023
16. ZABANIOTOU, A., IOANNIDOU, O., *Fuel*, **87**, 2008, p. 834
17. WHITE, P.J., JOHNSON, L.A., *Corn: Chemistry and Technology*, American Assoc. of Cereal Chemists, St. Paul, MN, USA, 2003
18. SINGH, V., JOHNSTON, D., *Advances in Food and Nutrition Research*, **48**, Elsevier Academic Press, San Diego, USA, 2004
19. DOBRE, T., PÂRVULESCU, O.C., IAVORSCHI, G., DOBREA, I., *Rev. Chim. (Bucharest)*, **57**, no.6, 2006, p. 658
20. DOBRE, T., PÂRVULESCU, O.C., IAVORSCHI, G., STOICA, A., STROESCU, M., *International Journal of Chemical Reactor Engineering*, **8**, 2010, p. 1968
21. DOBRE, T., PÂRVULESCU, O.C., CEATRĂ, L., STROESCU, M., IAVORSCHI, G., 6<sup>th</sup> European Meeting on Chemical Industry and Environment (EMChIE), May 17-19, Mechelen, Belgium, Conference Proceedings, **1**, 2010, p. 605
22. DOBRE, T., PÂRVULESCU, O.C., CEATRĂ, L., STOICA, A., IAVORSCHI, G., 19<sup>th</sup> International Congress of Chemical and Process Engineering (CHISA), August 28-September 1, Prague, Czechia, Conference Proceedings, **1**, 2010, p. 315
23. DOBRE, T., SANCHEZ, J., *Chemical Engineering - Modelling, Simulation and Similitude*, Wiley VCH, 2007

---

Manuscript received: 5.08.2010